

## **TWO-DIMENSIONAL STATIC DEFORMATION OF AN ORTHOTROPIC ELASTIC LAYERED HALF-SPACE DUE TO BLIND STRIKE-SLIP FAULT**

Shamta Chugh\*, Kuldip Singh\* and Dinesh Kumar Madan\*\*

\*Department of Mathematics

Guru Jambheshwar University of Science and Technology, Hisar-125001

\*\*Department of Mathematics

The Technological Institute of Textile and Sciences, Bhiwani-127021

### **ABSTRACT**

Closed-form analytical expressions for the deformation at any point of a horizontal orthotropic elastic layer of infinite lateral extent (coupling in different ways such as ‘welded’, ‘smooth-rigid’, or ‘rough-rigid’ to a base) due to a long blind strike-slip fault are obtained. The results obtained are generalization of the results for an isotropic medium. For different types of coupling, the effects of variations in depth on surface displacement are presented graphically. Also, at different depth levels, the variations of surface displacements with the horizontal distance from the inclined fault are compared to study the effects of different types of coupling. The results for the present model are compared with the corresponding results for a uniform orthotropic elastic half-space. It is observed that the displacement field varies more significantly in an orthotropic elastic layered half-space in comparison with a uniform orthotropic half-space. Numerically, the effect of anisotropy is also examined. It is found that anisotropy of the source half-space has a significant effect on the displacement at different depth levels.

**KEYWORDS:** Static Deformation, Surrounding Faults, Orthotropic Medium, Blind Fault, Strike-Slip

### **INTRODUCTION**

Many major faults reach and intersect with the surface of the earth. This intersection produces a linear feature called fault trace. Some faults do not reach the surface, however, and scientists refer to those as blind-faults. The devastating earthquake at Bam, Iran in 2003 is a well-documented case of blind strike-slip fault. It is common for earthquakes to occur on blind faults, which usually produce long-term surface effects by which their existence may be recognized (Talebian et al., 2004).

The upper part of the earth is anisotropic (Dziewonski and Anderson, 1981). Most anisotropic media of interest in seismology have at least one horizontal plane of symmetry. A plane of symmetry is a plane in which the elastic properties have reflection symmetry, and a medium with three mutually orthogonal planes of symmetry is known as orthorhombic. A large part of the earth is considered as having orthotropic symmetry (Crampin, 1994). The orthotropic symmetry of the upper mantle is believed to be caused by the orthorhombic crystals of olivine relative to the spreading centers (Hess, 1964). Orthorhombic symmetry is also expected to occur in sedimentary basins as a result of the combination of vertical cracks with a horizontal axis of symmetry and periodic thin-layer anisotropy with a vertical axis of symmetry (Bush and Crampin, 1987). In the case of one plane of symmetry, if the orthorhombic is horizontal, the symmetry is termed as orthotropic symmetry (Crampin, 1989). Since the orientation of stress in the crust is usually orthotropic, most symmetry systems in the earth’s crust also have orthotropic orientations. The orthotropy symmetry is also exhibited by olivine and orthopyroxenes which are the principal rock-forming minerals of the deep crust and the upper mantle.

The static deformation of a semi-infinite elastic isotropic medium due to a very long strike-slip fault has been studied by many researchers, e.g., Kasahara (1964), and Rybicki (1971, 1978). The results of these studies have been successfully applied to several earthquakes, e.g., 1906 San Andreas, 1927 Tango, 1948 Fukui, and 1966 Parkfield-Cholame. Analytical expressions for the surface deformation and internal deformation due to inclined shear and tensile faults in a homogeneous isotropic half-space are given by Okada (1985, 1992).

Using the body force equivalent of dislocation source as discussed by Burridge and Knopoff (1964) and Aki and Richards (1980), Pan (1989) obtained the response of a transversely isotropic layered medium to general dislocation sources. Using the results of Ben-Menahem and Singh (1968) and the method developed by Singh (1970), Rundle (1980) obtained the surface displacements due to a point source in a multilayered self-gravitating half-space.

Garg et al. (1996) obtained the representation of seismic sources causing antiplane-strain deformation of an orthotropic medium. Madan and Garg (1997) obtained analytical expressions for the displacements and stresses at any point of an orthotropic horizontal elastic layer, coupling in different ways such as ‘welded’, ‘smooth-rigid’, or ‘rough-rigid’ to a base, due to a very long inclined strike-slip fault.

Wang et al. (2003) introduced the techniques (i.e., orthonormalized Haskell propagator, analytical asymptotes, filter techniques, etc.) used to solve the stability and convergence problems when computing the Green functions. These techniques lead to small, fast and very accurate programs. Fernández and Rundle (2004) considered the problem of surface deformation arising from a fault in a semi-infinite, elastic-gravitational, and/or viscoelastic-gravitational, plane-layered medium which is subjected to an externally imposed gravitational acceleration. Fukahata and Matsu’ura (2006) used the correspondence principle of linear viscoelasticity to obtain the quasi-static deformation due to dislocation source in a multilayered elastic/viscoelastic half-space under gravity and also gave the equivalence theorem. Wang et al. (2006) presented a method and software to determine the surface and sub-surface deformations, as well as changes in the geoid and gravity, due to the common geophysical sources in a multilayered viscoelastic-gravitational half-space.

Recently, Rani and Singh (2005) obtained the static deformation of an isotropic semi-infinite elastic medium, consisting of a horizontal elastic layer in welded contact with an isotropic elastic half-space, due to a long blind strike-slip fault located in an elastic layer.

The present paper aims to study the static deformation of a horizontal orthotropic elastic layer of an infinite lateral extent, which is coupling in different ways to a base due to a long blind strike-slip fault situated in the elastic layer. The coupling of the layer with the base need not necessarily be ‘welded’; it may also be of the ‘smooth-rigid’ or ‘rough-rigid’ type. The different deformations of the horizontal orthotropic elastic layer corresponding to various types of its coupling with the base have been obtained analytically. In the study of Madan and Garg (1997), the depth  $d$  of the upper edge of the fault does not occur explicitly in the solution. Moreover, as the dip angle tends to zero, the fault approaches the surface of the earth. Therefore, their results cannot be used to study the deformation of a two-layer model caused by the deep strike-slip faults of small dip angles.

In the present formulation, depth  $d$  shows up explicitly in the solution. Therefore, the effects of variations in depth for a fixed dip with different types of coupling can be studied directly. The results obtained here are generalization of the results from an isotropic medium in the sense that the medium considered for the present work is orthotropic, which is more realistic than isotropic, and the results for the isotropic case can be derived from our results. Graphs showing the effects of variations in depth  $d$  on surface displacements for different types of coupling at different depth levels are presented. Numerically, the surface displacements for an orthotropic layered half-space are compared with the corresponding displacements for a uniform orthotropic elastic half-space. Also, at different depth levels, the surface displacements for different types of coupling (i.e., ‘welded’, ‘smooth’, and ‘rough’) are compared numerically.

### BASIC EQUATIONS

In the Cartesian coordinate system  $(x, y, z)$  the equations of equilibrium are

$$\tau_{ij,j} + F_i = 0 ; \quad i, j = 1, 2, 3 \tag{1}$$

where  $\tau_{ij}$  denotes the stress components and  $F_i$  represents the body forces per unit volume. The strain-displacement relations are

$$e_{11} = \frac{\partial u}{\partial x}, \quad e_{12} = \frac{1}{2} \left( \frac{\partial u}{\partial y} + \frac{\partial v}{\partial x} \right), \text{ etc.} \tag{2}$$

where  $u, v, w$  denote the displacement components along the  $x-, y-, z$ -axes, respectively.

For an orthotropic elastic medium, with coordinate planes coinciding with the planes of symmetry and with one plane of symmetry being horizontal, the stress-strain relations in matrix form are (Chung, 1996)

$$\begin{bmatrix} \tau_{11} \\ \tau_{22} \\ \tau_{33} \\ \tau_{23} \\ \tau_{13} \\ \tau_{12} \end{bmatrix} = \begin{bmatrix} c_{11} & c_{12} & c_{13} & 0 & 0 & 0 \\ c_{12} & c_{22} & c_{23} & 0 & 0 & 0 \\ c_{13} & c_{23} & c_{33} & 0 & 0 & 0 \\ 0 & 0 & 0 & c_{44} & 0 & 0 \\ 0 & 0 & 0 & 0 & c_{55} & 0 \\ 0 & 0 & 0 & 0 & 0 & c_{66} \end{bmatrix} \begin{bmatrix} e_{11} \\ e_{22} \\ e_{33} \\ 2e_{23} \\ 2e_{13} \\ 2e_{12} \end{bmatrix} \quad (3)$$

where the two-suffix quantity  $c_{ij}$  denotes the elastic constants of the medium. A transversely isotropic elastic medium, with the  $z$ -axis coinciding with the axis of symmetry, is a particular case of an orthotropic medium for which

$$c_{11} = c_{22}, \quad c_{23} = c_{13}, \quad c_{55} = c_{44}, \quad c_{66} = \frac{1}{2}(c_{11} - c_{12}) \quad (4)$$

and the number of independent elastic constants reduces from nine to five. For an elastic isotropic medium, these constants reduce to just two as given below,

$$\begin{aligned} c_{11} &= c_{22} = c_{33} = \lambda + 2\mu \\ c_{12} &= c_{13} = c_{23} = \lambda \\ c_{44} &= c_{55} = c_{66} = \mu \end{aligned} \quad (5)$$

where  $\lambda$  and  $\mu$  are the Lamé's constants.

There are two distinct approaches by which one can represent a source in the seismological boundary value problems. In the first approach, one uses a body force equivalent to the source. Consequently, the equations of motion become inhomogeneous due to the presence of the source term. In the second approach, the source is removed from the equation of motion, which becomes homogeneous, but appears instead as a source condition. This source condition corresponds to the jump in the displacement and stress components across a coordinate surface passing through the source. With reference to the second approach, the equilibrium equations for zero body forces are given by

$$\frac{\partial \tau_{11}}{\partial x} + \frac{\partial \tau_{12}}{\partial y} + \frac{\partial \tau_{13}}{\partial z} = 0 \quad (6)$$

$$\frac{\partial \tau_{21}}{\partial x} + \frac{\partial \tau_{22}}{\partial y} + \frac{\partial \tau_{23}}{\partial z} = 0 \quad (7)$$

$$\frac{\partial \tau_{31}}{\partial x} + \frac{\partial \tau_{32}}{\partial y} + \frac{\partial \tau_{33}}{\partial z} = 0 \quad (8)$$

Let the elastic medium under consideration be under the conditions of antiplane-strain deformation in the  $yz$ -plane due to a very long strike-slip dislocation parallel to the  $x$ -axis. In this case, the displacement vector is parallel to the  $x$ -axis (or the direction of the fault strike) and  $\partial(\cdot)/\partial x \equiv 0$ . Thus, under the state of antiplane-strain deformation,  $v = w = 0$ , and  $u = u(y, z)$ . The non-zero stresses can be written as

$$\tau_{12} = c\alpha^2 \frac{\partial u}{\partial y}, \quad \tau_{13} = c \frac{\partial u}{\partial z} \quad (9)$$

where

$$c = c_{55}, \quad c_{66} = c\alpha^2 \quad (10)$$

and  $\alpha$  and  $c$  are real positive numbers. In the case of an isotropic elastic medium,  $c = \mu$  and  $\alpha = 1$ .

The equilibrium equations (i.e., Equations (7) and (8)) are identically satisfied for the antiplane-strain deformation. In that case, Equation (6) is reduced to

$$\frac{\partial^2 u}{\partial y^2} + \frac{1}{\alpha^2} \frac{\partial^2 u}{\partial z^2} = 0 \tag{11}$$

and the source condition to be satisfied by the resulting tractions becomes (Maruyama, 1966)

$$\oint \tau_{1k} \nu_k d\sigma = F \tag{12}$$

where  $F$  is the magnitude of the force (per unit length) acting at the point  $(\xi_2, \xi_3)$  in an infinite homogeneous orthotropic elastic medium in the positive  $x$ -direction, and  $\nu_k$  denotes the direction cosines of the exterior normal.

The solution of Equation (11) using the source boundary condition of Equation (12) becomes (Garg et al., 1996)

$$u = \frac{-F}{4\pi\alpha c} \log \left[ (y - \xi_2)^2 + \alpha^2 (z - \xi_3)^2 \right] \tag{13}$$

for the displacement parallel to the  $x$ -axis and at any point  $(y, z)$  of an orthotropic elastic infinite medium, due to a line source, which is parallel to the  $x$ -axis and is passing through the point  $(\xi_2, \xi_3)$ .

### 1. Single Couples ( $xy$ ) and ( $xz$ )

At the point  $(\xi_2, \xi_3)$ , there acts a two-dimensional line source—either a single couple ( $xy$ ) or a single couple ( $xz$ ). The displacements  $u^{(xy)}$  and  $u^{(xz)}$  parallel to the  $x$ -axis, due to the single couple ( $xy$ ) of moment  $F_{xy}$  and due to the single couple ( $xz$ ) of moment  $F_{xz}$ , respectively, are found to be

$$u^{(xy)} = \frac{F_{xy}}{2\pi\alpha c} \int_0^\infty e^{-k\alpha|z-\xi_3|} \sin k(y - \xi_2) dk \tag{14}$$

$$u^{(xz)} = \pm \frac{F_{xz}}{2\pi\alpha c} \int_0^\infty e^{-k\alpha|z-\xi_3|} \cos k(y - \xi_2) dk \tag{15}$$

These displacements (parallel to the  $x$ -axis, and due to the line source of a single couple ( $xy$ ) or ( $xz$ )) can be unified into the following integral:

$$u_0 = \int_0^\infty \left[ A_0 \sin k(y - \xi_2) + B_0 \cos k(y - \xi_2) \right] e^{-\alpha k|z-\xi_3|} dk \tag{16}$$

The source coefficients  $A_0$  and  $B_0$  for various two-dimensional buried sources are given in Table 1.

## FORMULATION AND SOLUTION OF THE PROBLEM

We consider a semi-infinite medium consisting of a homogeneous orthotropic elastic horizontal layer of thickness  $H$  lying over a homogeneous orthotropic elastic half-space. The origin of the Cartesian coordinate system  $(x, y, z)$  is placed at the upper boundary of the semi-infinite medium with the  $z$ -axis vertically downwards (see Figure 1). The layer, therefore, occupies the region  $0 \leq z < H$ . It is assumed that an orthotropic elastic horizontal layer is coupling in different ways such as ‘welded’, ‘smooth-rigid’, or ‘rough-rigid’ to a base. We consider an inclined strike-slip fault of finite width  $L$  with an arbitrary dip angle  $\delta$ , which lies completely in the orthotropic horizontal elastic layer and whose upper edge is at depth  $d$  below the earth surface.

The boundary surface  $z = 0$  is a horizontal plane and a plane of elastic symmetry. It is further assumed that this plane is traction free, so that

$$\tau_{13}|_{z=0} = 0 \tag{17}$$

and the boundary conditions at the interface  $z = H$  for different types of coupling are

$$u|_{z=H^+} = u|_{z=H^-}, \quad \tau_{13}|_{z=H^+} = \tau_{13}|_{z=H^-} \tag{18}$$

for the welded contact,

$$\tau_{13}|_{z=H} = 0 \tag{19}$$

for the smooth-rigid contact, and

$$u|_{z=H} = 0 \tag{20}$$

for the rough-rigid contact.

**Table 1: Source Coefficients for Various Seismic Sources**

Source	$A_0$	$B_0$
Single Couple (12)	$\frac{F_{xy}}{2\pi\alpha c}$	0
Single Couple (13)	0	$\pm \frac{F_{xz}}{2\pi c}$

The upper sign is for  $z > \xi_3$  and the lower sign for  $z < \xi_3$ .  
 $F_{xy}$  and  $F_{xz}$  are, respectively, the moments of couples (xy) and (xz).

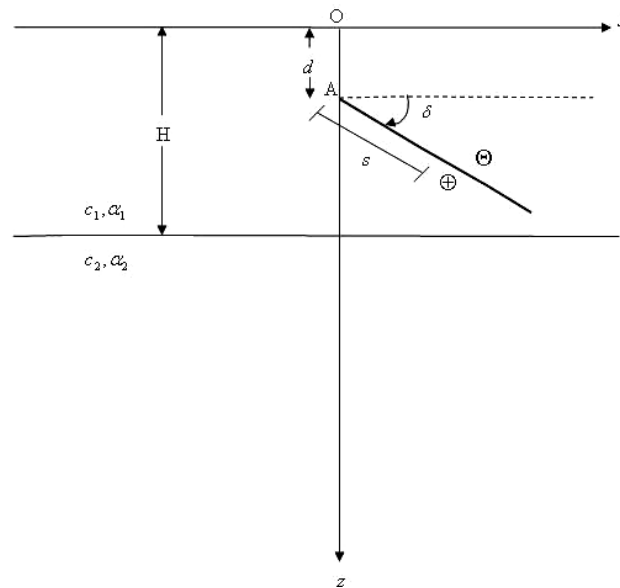


Fig. 1 Geometry of an inclined strike-slip fault of finite width  $L$  situated in an orthotropic layer of uniform thickness  $H$  lying over a half-space (the displacement discontinuity on the inclined fault is parallel to the  $x$ -axis; the symbol  $\oplus$  indicates displacement in the direction of the  $x$ -axis and the symbol  $\ominus$  in the opposite direction;  $d$  is the depth of the upper edge  $A$  of the fault and  $\delta$  is the dip angle;  $s$  is the distance from the upper edge of the fault measured in the dip direction)

For a line source acting at the point  $(\xi_2, \xi_3)$  of the layer, suitable expressions for the horizontal displacements parallel to the line source and satisfying Equation (11), in the layer and in the half-space, are

$$u^{(1)} = u_0 + \int_0^{\infty} [A_1 \sin k(y - \xi_2) + B_1 \cos k(y - \xi_2)] e^{-\alpha_1 k z} dk + \int_0^{\infty} [C_1 \sin k(y - \xi_2) + C_1 \cos k(y - \xi_2)] e^{\alpha_1 k z} dk \quad (21)$$

for  $0 \leq z < H$ , and

$$u^{(2)} = \int_0^{\infty} [A_2 \sin k(y - \xi_2) + B_2 \cos k(y - \xi_2)] e^{-\alpha_2 k z} dk \quad (22)$$

for  $z > H$ . Here, the superscript (1) is for the layer and superscript (2) for the half-space. The coefficients  $A_1, B_1$ , etc. for each type of coupling can be determined by using the boundary conditions of Equations (17)–(20).

### 1. Inclined Strike-Slip Fault

The displacement field due to a very long strike-slip line fault of arbitrary dip  $\delta$  can be expressed in terms of two fields, one due to a horizontal strike-slip fault and the other due to a vertical strike-slip fault, in the form (Singh and Garg, 1985)

$$u = u^{(HS)} \cos \delta + u^{(VS)} \sin \delta \quad (23)$$

where  $u^{(HS)}$  is the displacement for the horizontal strike-slip fault, and  $u^{(VS)}$  is the displacement for the vertical strike-slip fault.

Using the results for the horizontal and vertical strike-slip faults, as obtained earlier by Garg et al. (1996), we obtain the following expressions for the displacements due to the ‘welded’ contact, which is parallel to the  $x$ -axis, due to a long strike-slip fault of finite width  $L$ :

$$u^{(1)} = \frac{b\alpha_1}{2\pi} \left\{ \sum_{n=0}^{\infty} T^n \left[ \frac{(2nH + z - \xi_3) \cos \delta - (y - \xi_2) \sin \delta}{(y - \xi_2)^2 + [\alpha_1(2nH + z - \xi_3)]^2} - \frac{(2nH + z + \xi_3) \cos \delta + (y - \xi_2) \sin \delta}{(y - \xi_2)^2 + [\alpha_1(2nH + z + \xi_3)]^2} \right] + \sum_{n=1}^{\infty} T^n \left[ \frac{(2nH - z - \xi_3) \cos \delta - (y - \xi_2) \sin \delta}{(y - \xi_2)^2 + [\alpha_1(2nH - z - \xi_3)]^2} - \frac{(2nH - z + \xi_3) \cos \delta + (y - \xi_2) \sin \delta}{(y - \xi_2)^2 + [\alpha_1(2nH - z + \xi_3)]^2} \right] \right\} ds \quad (24)$$

for  $0 \leq z < H$ , and

$$u^{(2)} = -\frac{b}{2\pi} \left\{ \sum_{n=0}^{\infty} (1+T) T^n \left[ \frac{[\alpha_1(2nH + H + \xi_3) + \alpha_2(z - H)] \cos \delta + \alpha_1(y - \xi_2) \sin \delta}{(y - \xi_2)^2 + [\alpha_1(2nH + H + \xi_3) + \alpha_2(z - H)]^2} - \frac{[\alpha_1(2nH + H - \xi_3) + \alpha_2(z - H)] \cos \delta - \alpha_1(y - \xi_2) \sin \delta}{(y - \xi_2)^2 + [\alpha_1(2nH + H - \xi_3) + \alpha_2(z - H)]^2} \right] \right\} ds \quad (25)$$

for  $z > H$ , where  $b$  is the uniform slip;  $ds$  is the infinitesimal width of the line dislocation (parallel to the  $x$ -axis);  $c_1, \alpha_1$  and  $c_2, \alpha_2$  are the elastic constants for the orthotropic elastic layer and the half-space, respectively;

$$T = \frac{1-m}{1+m}, \quad m = \frac{c_2 \alpha_2}{c_1 \alpha_1} \quad (26)$$

and  $s$  is the distance from the upper edge of the fault measured in the down-dip direction.

On substituting  $\xi_2 = s \cos \delta$  and  $\xi_3 = d + s \sin \delta$  into Equations (24) and (25) and then on integrating over  $s$  from 0 to  $L$ , we obtain the following expressions for the displacements and stresses:

$$u^{(1)} = \frac{b}{2\pi} \left[ \sum_{n=0}^{\infty} T^n \left\{ \tan^{-1} \frac{T_2}{T_1} - \tan^{-1} \frac{T_4}{T_3} \right\} + \sum_{n=1}^{\infty} T^n \left\{ \tan^{-1} \frac{T_6}{T_5} - \tan^{-1} \frac{T_8}{T_7} \right\} \right] \Big|_0^L \quad (27)$$

$$\tau_{12}^{(1)} = \frac{bc_1\alpha_1^3 T_0}{2\pi} \left[ \sum_{n=0}^{\infty} T^n \left\{ \frac{2nH + z + d + s \sin \delta}{T_3^2 + T_4^2} - \frac{2nH + z - d - s \sin \delta}{T_1^2 + T_2^2} \right\} + \sum_{n=1}^{\infty} T^n \left\{ \frac{2nH - z + d + s \sin \delta}{T_7^2 + T_8^2} - \frac{2nH - z - d - s \sin \delta}{T_5^2 + T_6^2} \right\} \right] \Big|_0^L \quad (28)$$

$$\tau_{13}^{(1)} = \frac{bc_1\alpha_1 T_0}{2\pi} \left[ \sum_{n=0}^{\infty} T^n \left\{ \frac{y - s \cos \delta}{T_1^2 + T_2^2} - \frac{y - s \cos \delta}{T_3^2 + T_4^2} \right\} - \sum_{n=1}^{\infty} T^n \left\{ \frac{y - s \cos \delta}{T_5^2 + T_6^2} - \frac{y - s \cos \delta}{T_7^2 + T_8^2} \right\} \right] \Big|_0^L \quad (29)$$

for  $0 \leq z < H$ , and

$$u^{(2)} = -\frac{b}{2\pi} \left[ \sum_{n=0}^{\infty} (1+T) T^n \left\{ \tan^{-1} \frac{T_{10}}{T_9} + \tan^{-1} \frac{T_{12}}{T_{11}} \right\} \right] \Big|_0^L \quad (30)$$

$$\tau_{12}^{(2)} = \frac{bc_2\alpha_2^2 T_0}{2\pi} \left[ \sum_{n=0}^{\infty} (1+T) T^n \left\{ \frac{[\alpha_1(2nH + H + d) + \alpha_2(z - H)] + \alpha_1 s \sin \delta}{T_9^2 + T_{10}^2} - \frac{[\alpha_1(2nH + H - d) + \alpha_2(z - H)] - \alpha_1 s \sin \delta}{T_{11}^2 + T_{12}^2} \right\} \right] \Big|_0^L \quad (31)$$

$$\tau_{13}^{(2)} = \frac{bc_2\alpha_1 T_0}{2\pi} \left[ \sum_{n=0}^{\infty} (1+T) T^n \left\{ \frac{y - s \cos \delta}{T_{11}^2 + T_{12}^2} - \frac{y - s \cos \delta}{T_9^2 + T_{10}^2} \right\} \right] \Big|_0^L \quad (32)$$

for  $z > H$ , where

$$\begin{aligned} T_0 &= (\cos^2 \delta + \alpha_1^2 \sin^2 \delta); & T_1 &= \alpha_1 [(2nH + z - d) \cos \delta - y \sin \delta] \\ T_2 &= T_0 s - [y \cos \delta + \alpha_1^2 (2nH + z - d) \sin \delta]; & T_3 &= \alpha_1 [(2nH + z + d) \cos \delta + y \sin \delta] \\ T_4 &= T_0 s - [y \cos \delta - \alpha_1^2 (2nH + z + d) \sin \delta]; & T_5 &= \alpha_1 [(2nH - z - d) \cos \delta - y \sin \delta] \\ T_6 &= T_0 s - [y \cos \delta + \alpha_1^2 (2nH - z - d) \sin \delta]; & T_7 &= \alpha_1 [(2nH - z + d) \cos \delta + y \sin \delta] \\ T_8 &= T_0 s - [y \cos \delta - \alpha_1^2 (2nH - z + d) \sin \delta] \\ T_9 &= \alpha_1 y \sin \delta + [\alpha_1(2nH + H + d) + \alpha_2(z - H)] \cos \delta \\ T_{10} &= T_0 s - [y \cos \delta - \{\alpha_1(2nH + H + d) + \alpha_2(z - H)\} \alpha_1 \sin \delta] \\ T_{11} &= \alpha_1 y \sin \delta - [\alpha_1(2nH + H - d) + \alpha_2(z - H)] \cos \delta \\ T_{12} &= T_0 s - [y \cos \delta + \{\alpha_1(2nH + H - d) + \alpha_2(z - H)\} \alpha_1 \sin \delta] \end{aligned} \quad (33)$$

and

$$f(s) \Big|_0^L = f(L) - f(0) \quad (34)$$

It has been verified that the boundary conditions in Equation (18) are identically satisfied by Equations (27)–(32).

On putting  $\alpha_1 = \alpha_2 = \alpha$ ,  $c_1 = c_2 = c$ , and  $T = 0$  in Equation (27) or (30), we get the displacement field due to a very long blind strike-slip fault of finite width  $L$  in a uniform orthotropic elastic half-space:

$$u = \frac{b}{2\pi} \left[ \tan^{-1} \frac{(\cos^2 \delta + \alpha^2 \sin^2 \delta) s - [y \cos \delta + \alpha^2 (z-d) \sin \delta]}{\alpha [(z-d) \cos \delta - y \sin \delta]} - \tan^{-1} \frac{(\cos^2 \delta + \alpha^2 \sin^2 \delta) s - [y \cos \delta - \alpha^2 (z+d) \sin \delta]}{\alpha [(z+d) \cos \delta + y \sin \delta]} \right] \Bigg|_0^L \quad (35)$$

The corresponding stresses can be obtained on using Equation (35) in Equation (9).

## 2. Particular Cases

### 2.1 Smooth-Rigid Contact

When the interface  $z = H$  between the layer and the half-space is ‘smooth-rigid’, on taking  $m = 0$ , i.e.,  $T = 1$ , in Equations (27) and (30), we obtain the corresponding displacement field as

$$u^{(1)} = \frac{b}{2\pi} \left[ \tan^{-1} \frac{(\cos^2 \delta + \alpha_1^2 \sin^2 \delta) s - [y \cos \delta + \alpha_1^2 (z-d) \sin \delta]}{\alpha_1 [(z-d) \cos \delta - y \sin \delta]} - \tan^{-1} \frac{(\cos^2 \delta + \alpha_1^2 \sin^2 \delta) s - [y \cos \delta - \alpha_1^2 (z+d) \sin \delta]}{\alpha_1 [(z+d) \cos \delta + y \sin \delta]} + \sum_{n=1}^{\infty} \left\{ \tan^{-1} \frac{T_2}{T_1} - \tan^{-1} \frac{T_4}{T_3} + \tan^{-1} \frac{T_6}{T_5} - \tan^{-1} \frac{T_8}{T_7} \right\} \right] \Bigg|_0^L \quad (36)$$

for  $0 \leq z < H$ , and

$$u^{(2)} = -\frac{b}{\pi} \left[ \tan^{-1} \frac{(\cos^2 \delta + \alpha_1^2 \sin^2 \delta) s - [y \cos \delta - \{\alpha_1 (H+d) + \alpha_2 (z-H)\} \alpha_1 \sin \delta]}{\alpha_1 y \sin \delta + [\alpha_1 (H+d) + \alpha_2 (z-H)] \cos \delta} + \tan^{-1} \frac{(\cos^2 \delta + \alpha_1^2 \sin^2 \delta) s - [y \cos \delta + \{\alpha_1 (H-d) + \alpha_2 (z-H)\} \alpha_1 \sin \delta]}{\alpha_1 y \sin \delta - [\alpha_1 (H-d) + \alpha_2 (z-H)] \cos \delta} + \sum_{n=1}^{\infty} \left\{ \tan^{-1} \frac{T_{10}}{T_9} + \tan^{-1} \frac{T_{12}}{T_{11}} \right\} \right] \Bigg|_0^L \quad (37)$$

for  $z > H$ .

### 2.2 Rough-Rigid Contact

When the interface  $z = H$  between the layer and the half-space is ‘rough-rigid’, on letting  $m \rightarrow \infty$ , i.e.,  $T = -1$ , in Equations (27) and (30), we get the displacement field as

$$u^{(1)} = \frac{b}{2\pi} \left[ \tan^{-1} \frac{(\cos^2 \delta + \alpha_1^2 \sin^2 \delta) s - [y \cos \delta + \alpha_1^2 (z-d) \sin \delta]}{\alpha_1 [(z-d) \cos \delta - y \sin \delta]} - \tan^{-1} \frac{(\cos^2 \delta + \alpha_1^2 \sin^2 \delta) s - [y \cos \delta - \alpha_1^2 (z+d) \sin \delta]}{\alpha_1 [(z+d) \cos \delta + y \sin \delta]} \right] \quad (38)$$



$$+ \sum_{n=1}^{\infty} (-1)^n \left\{ \tan^{-1} \frac{T_2}{T_1} - \tan^{-1} \frac{T_4}{T_3} + \tan^{-1} \frac{T_6}{T_5} - \tan^{-1} \frac{T_8}{T_7} \right\} \Bigg|_0^L$$

for  $0 \leq z < H$ , and

$$u^{(2)} = 0 \tag{39}$$

for  $z > H$ .

### 2.3 Isotropic Case

The results for the corresponding problem for an isotropic case can be obtained as a particular case of the results given in Equations (27) and (30) by taking  $\alpha_1 = \alpha_2 = 1$ ,  $c_1 = \mu_1$ ,  $c_2 = \mu_2$ , and  $T = (\mu_1 - \mu_2) / (\mu_1 + \mu_2)$ . The results so obtained coincide with the results obtained by Rani and Singh (2005).

## NUMERICAL RESULTS

In this section, we examine the effect of the variation in the depth  $d$  of the upper edge of the fault on the displacement field caused by a uniform slip along a very long strike-slip fault, for each type of coupling between the orthotropic elastic layer lying over an orthotropic elastic half-space and the base (see Figure 1). Further, we compare the displacement field, due to a very long strike-slip fault of finite width  $L$  with its edge at distance  $d$  from the surface which is located in the orthotropic elastic layer and is in ‘welded’ contact with the orthotropic half-space along the horizontal plane, with the corresponding displacement field for a uniform orthotropic elastic half-space. The effects of different types of coupling between the orthotropic elastic layer and the base upon the displacement  $u^{(1)}$  with the horizontal distance  $y$  from the fault are also examined.

We define the dimensionless displacement and distance as  $U^{(1)} = u^{(1)} / b$  and  $Y = y / H$ , respectively. Further, we assume  $L = H / 2$  and  $\gamma = d / H$ . For the orthotropic layered medium, we use the values of the elastic constants,  $\alpha_1 = 0.9824$ ,  $c_1 = 2.87 \times 10^{11}$  dynes/cm<sup>2</sup> (28.7 GPa) for the material baryte, as given by Love (1944), and  $\alpha_2 = 0.9894$ ,  $c_2 = 8.10 \times 10^{11}$  dynes/cm<sup>2</sup> (81 GPa) for the material olivine, as given by Verma (1960). In the case of a uniform orthotropic elastic half-space, we consider the material to be baryte. The explicit analytical expressions describing the elastic field involve infinite series. The infinite series appearing at the right hand side of Equations (27) and (30) converge very rapidly. In numerical computations, it is found that the first twenty terms of the infinite series, which appear in the closed-form expression for the displacement  $u$ , are adequate and, therefore, the series is truncated after the first twenty terms.

Figures 2(a)–2(c) exhibit the variations of the dimensionless surface displacement  $U^{(1)}$  with the dimensionless horizontal distance  $Y$  from the upper edge of the fault for four different values of  $\gamma$  ( $= 0, 1/4, 2/3, 1$  for the ‘welded’, ‘smooth’, ‘rough’ contacts, respectively) at the dip angle  $\delta = 30^\circ, 15^\circ, \text{ and } 60^\circ$ , respectively. We observe that the displacement for the surface-breaking fault (i.e.,  $\gamma = 0$ ) is discontinuous at  $Y = 0$ , while it is continuous at all values of  $Y$  for  $\gamma = 1/4, 2/3, 1$ , for each type of coupling between the orthotropic elastic layer and the orthotropic elastic half-space. It follows that for the surface-breaking fault (i.e.,  $\gamma = 0$ ), the amount of discontinuity in the horizontal displacement at the point  $Y = 0$  is unity for all possible types of coupling.

Next, in Figures 3(a)–3(f), we compare the surface displacement due to a very long strike-slip fault for an orthotropic layered elastic medium with the corresponding displacement for a uniform orthotropic elastic half-space. In the Figures 3(a)–3(d), the dimensionless horizontal displacements parallel to the fault at  $\delta = 30^\circ$  have been shown for four different depth levels  $\gamma = 1/4, 1/2, 2/3, 1$ , respectively. Figures 3(e) and 3(f) show the variations of  $U^{(1)}$  due to a long vertical strike-slip fault at different depth levels  $\gamma = 1/2$  and  $2/3$ , respectively.

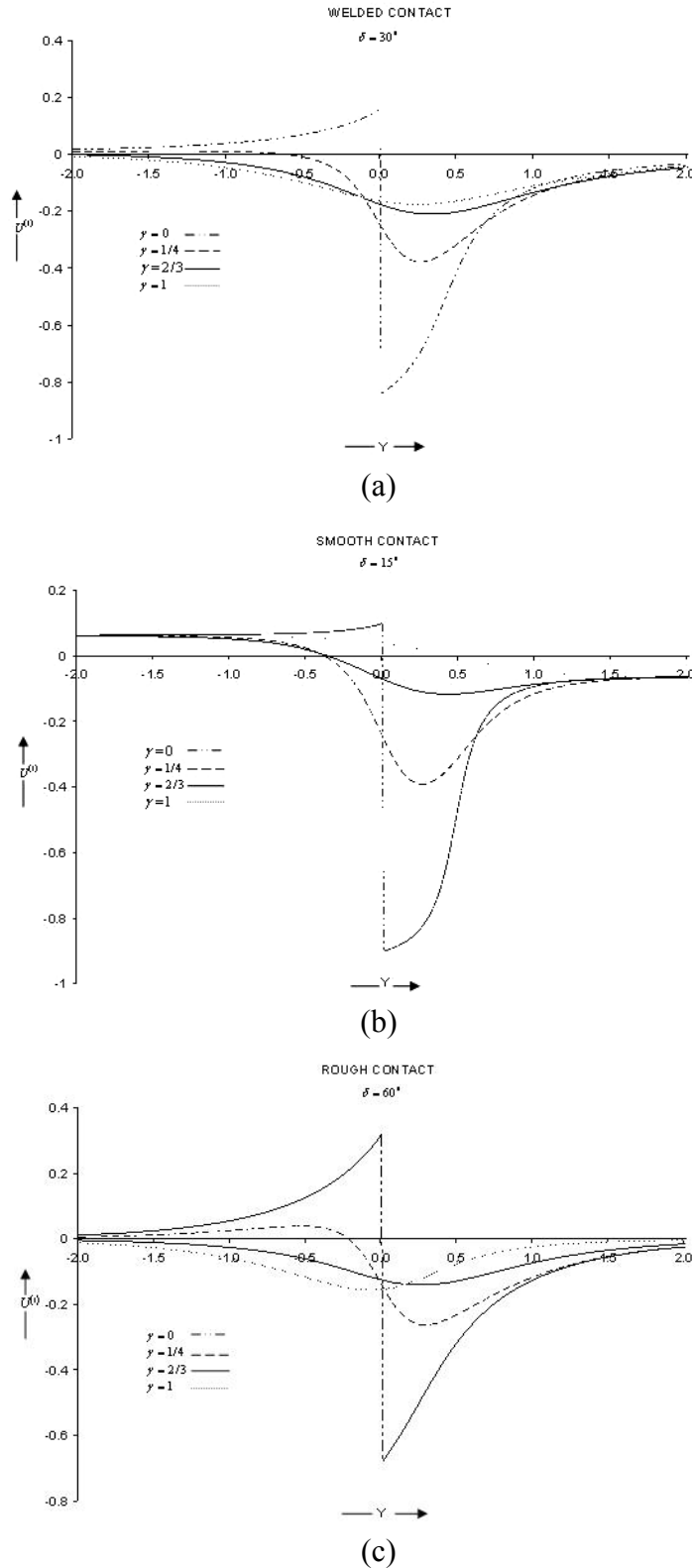


Fig. 2 (a) Variation of dimensionless surface displacement  $U^{(1)}$ , due to ‘welded’ contact, with the dimensionless horizontal distance  $Y$  from the upper edge of the fault for depth  $\gamma = 0, 1/4, 2/3, 1$  and dip angle  $\delta = 30^\circ$ ; (b) Variation of  $U^{(1)}$ , due to ‘smooth’ contact, with  $Y$  for  $\gamma = 0, 1/4, 2/3, 1$  and dip angle  $\delta = 15^\circ$ ; (c) Variation of  $U^{(1)}$ , due to ‘rough’ contact, with  $Y$  for  $\gamma = 0, 1/4, 2/3, 1$  and dip angle  $\delta = 60^\circ$

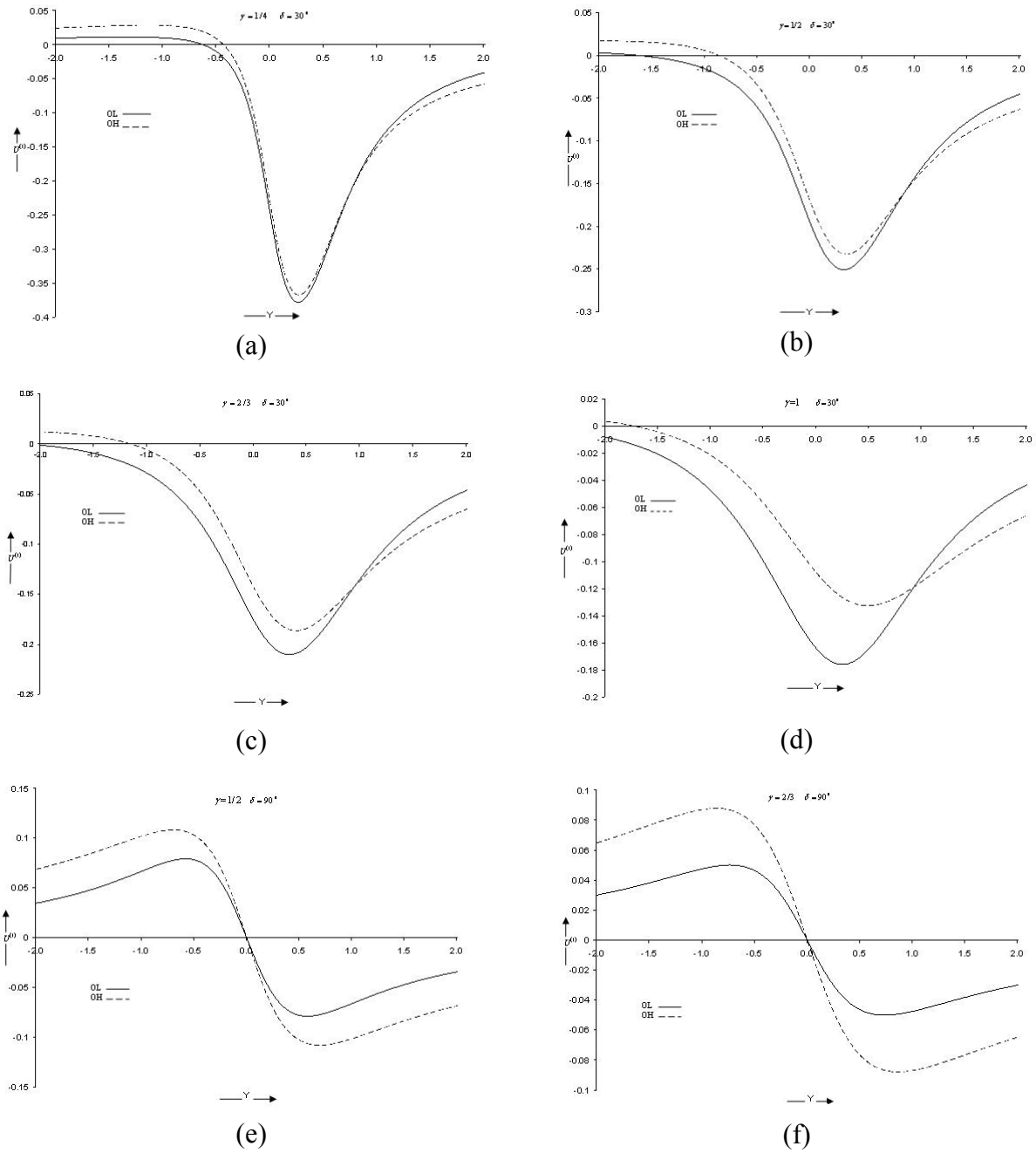


Fig. 3 (a) Variations of dimensionless surface displacement  $U^{(1)}$  due to a very long strike-slip fault for an orthotropic elastic layered half-space (OL) and for a uniform orthotropic elastic half-space (OH) with the dimensionless horizontal distance  $Y$  from the upper edge of the fault for depth  $\gamma = 1/4$  and dip angle  $\delta = 30^\circ$ ; (b) Variations of  $U^{(1)}$  with  $Y$  for an orthotropic elastic layered half-space (OL) and uniform orthotropic elastic half-space (OH) for  $\gamma = 1/2$  and  $\delta = 30^\circ$ ; (c) Variations of  $U^{(1)}$  with  $Y$  for an orthotropic elastic layered half-space (OL) and uniform orthotropic elastic half-space (OH) for  $\gamma = 2/3$  and  $\delta = 30^\circ$ ; (d) Variations of  $U^{(1)}$  with  $Y$  for an orthotropic elastic layered half-space (OL) and uniform orthotropic elastic half-space (OH) for  $\gamma = 1$  and  $\delta = 30^\circ$ ; (e) Variations of  $U^{(1)}$  with  $Y$  for an orthotropic elastic layered half-space (OL) and uniform orthotropic elastic half-space (OH) for  $\gamma = 1/2$  and  $\delta = 90^\circ$ ; (f) Variations of  $U^{(1)}$  with  $Y$  for an orthotropic elastic layered half-space (OL) and uniform orthotropic elastic half-space (OH) for  $\gamma = 2/3$  and  $\delta = 90^\circ$

From all of these figures it is found that as the depth increases, the discrepancy between the displacements due to a very long strike-slip fault for an orthotropic elastic layered half-space model and for a uniform orthotropic elastic half-space model increases. We also note that the horizontal displacement varies quite significantly in the orthotropic elastic layered model as well as in the uniform orthotropic elastic half-space model.

Curves representing the dimensionless horizontal displacement at different points of the orthotropic elastic layer, corresponding to different types of coupling, are shown in Figures 4(a)–4(c) at different combinations of depth levels and dip angles. In each figure, we observe that the displacements due to ‘welded’ coupling lie between the corresponding values due to the ‘smooth-rigid’ and ‘rough-rigid’ couplings.

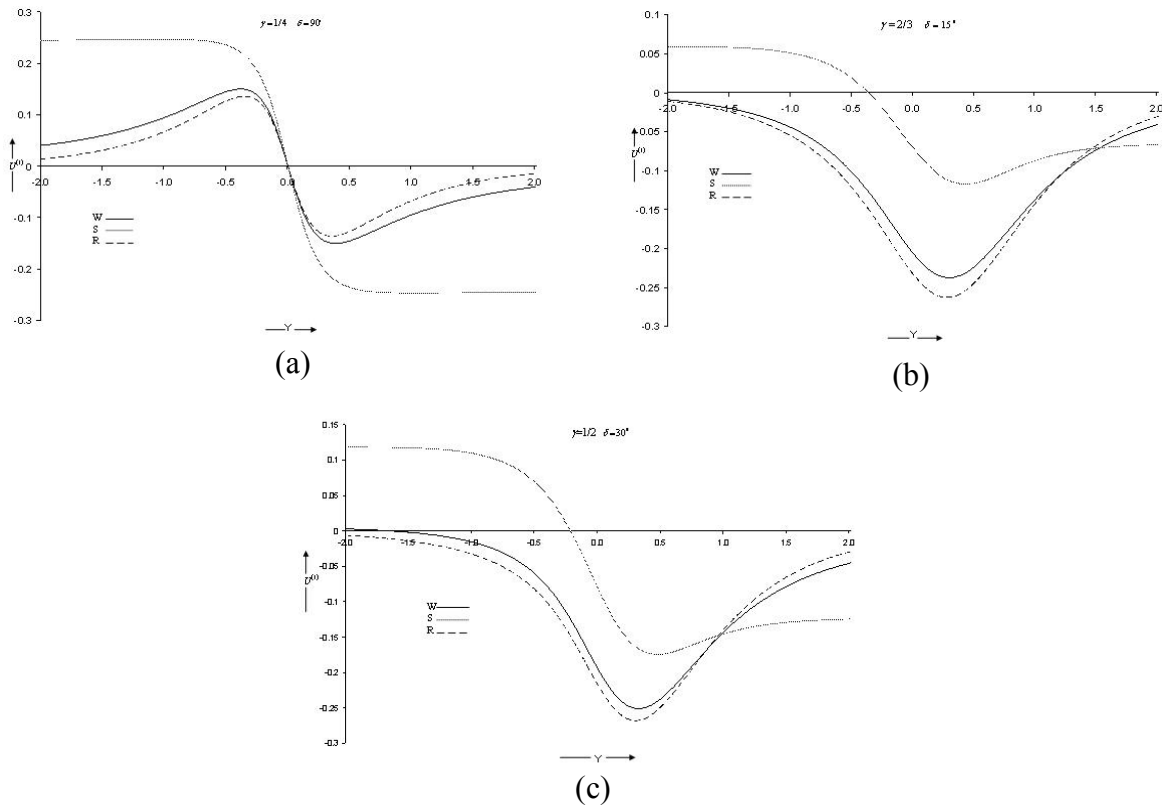


Fig. 4 (a) Variation of  $U^{(1)}$ , due to ‘welded’ contact, with the dimensionless horizontal distance  $Y$  from the upper edge of the fault for depth  $\gamma = 1/4$  and  $\delta = 30^\circ$  (W denotes ‘welded’, S ‘smooth-rigid’, and R ‘rough-rigid’ coupling); (b) Variation of  $U^{(1)}$  with  $Y$  for  $\gamma = 2/3$  and  $\delta = 15^\circ$  (W denotes ‘welded’, S ‘smooth-rigid’, and R ‘rough-rigid’ coupling); (c) Variation of  $U^{(1)}$  with  $Y$  for  $\gamma = 1/2$  and  $\delta = 30^\circ$  (W denotes ‘welded’, S ‘smooth-rigid’, and R ‘rough-rigid’ coupling)

Figures 5(a)–5(d) show the effect of anisotropy upon the variation of displacement parallel to the fault with the horizontal distance from the fault, by varying the anisotropy parameter  $\alpha$  of the elastic medium at different combinations of depth levels and angles. For an isotropic elastic medium of any kind, we have  $\alpha = 1$ . For an anisotropic medium, we consider three possibilities:  $\alpha = 0.25, 0.5, 0.75$ . In Figures 5(a) and 5(b), and in Figures 5(c) and 5(d), four curves corresponding to the anisotropy parameter  $\alpha = 0.25, 0.5, 0.75$ , and 1 (isotropic medium) are drawn at the dip angle  $\delta$  equal to  $15^\circ$  and  $30^\circ$ , respectively, for the depth levels,  $\gamma = 1/4, 1/2, 2/3, 1$ . We note that the anisotropy parameter  $\alpha$  of the source half-space has a significant effect on the displacement field.

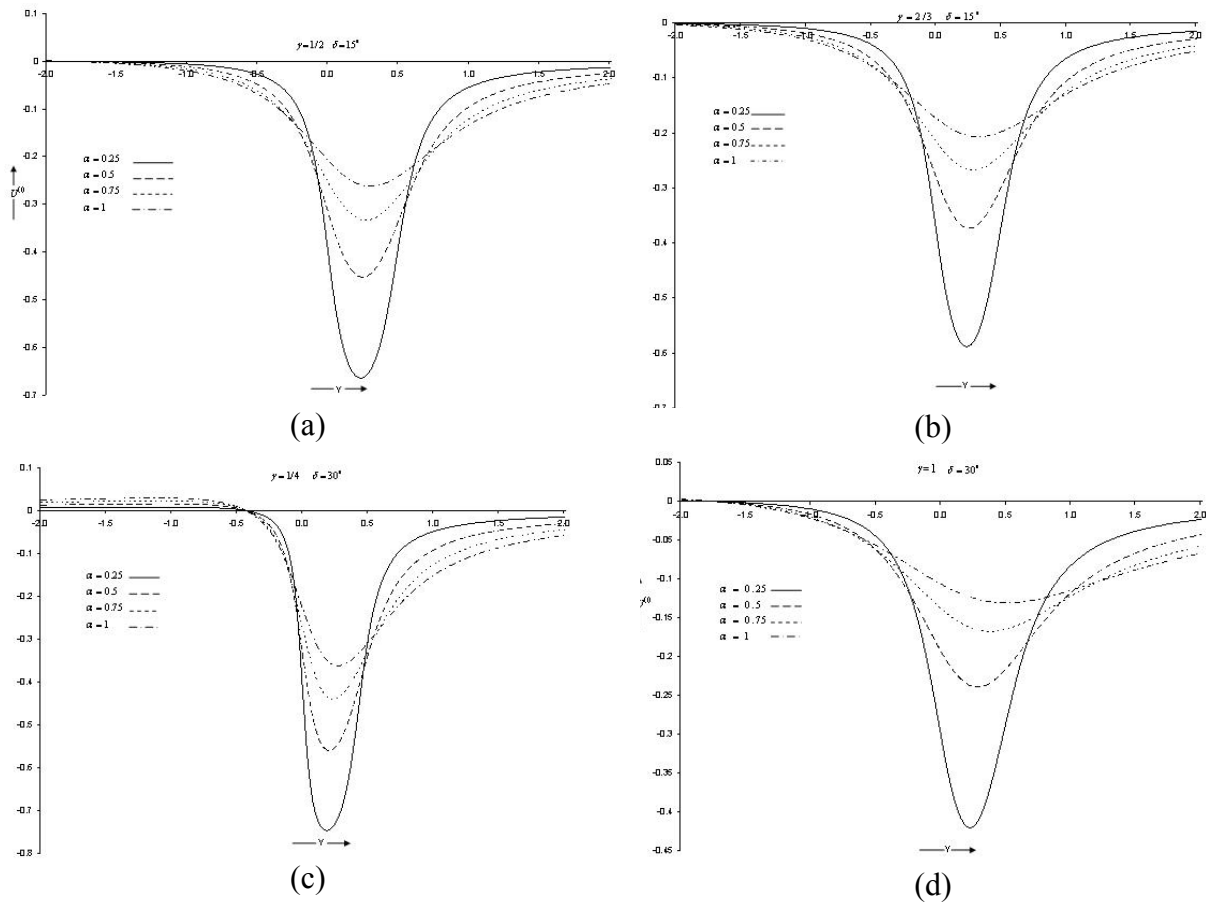


Fig. 5 (a) Variations of  $U^{(1)}$  with  $Y$  for uniform half-space with the anisotropy parameter  $\alpha = 0.25, 0.5, 0.75,$  and  $1$  (isotropic medium), for  $\gamma = 1/2$  and  $\delta = 15^\circ$ ; (b) Variations of  $U^{(1)}$  with  $Y$  for  $\alpha = 0.25, 0.5, 0.75, 1,$  with  $\gamma = 2/3$  and  $\delta = 15^\circ$ ; (c) Variations of  $U^{(1)}$  with  $Y$  for  $\alpha = 0.25, 0.5, 0.75, 1,$  with  $\gamma = 1/4$  and  $\delta = 30^\circ$ ; (d) Variations of  $U^{(1)}$  with  $Y$  for  $\alpha = 0.25, 0.5, 0.75, 1,$  with  $\gamma = 1$  and  $\delta = 30^\circ$

**DISCUSSION AND CONCLUSIONS**

In the present study, we have obtained analytical expressions for the static displacements and stresses at an arbitrary point of an orthotropic elastic layered medium, which are caused by a very long strike-slip fault situated at depth  $d$  in an orthotropic elastic layer. We have considered three cases of the contact between the layer and the half-space: ‘welded’, ‘smooth’, and ‘rough’. The displacement field for an orthotropic elastic layered half-space has also been compared numerically with the displacement field for a uniform orthotropic elastic half-space. It has been found that as the depth level increases, the difference between the two displacements also increases. Further, we have compared the displacement fields for different types of coupling, namely, ‘welded’, ‘smooth’, and ‘rough’, between the layer and the half-space. The effect of variation in depth  $d$  of the upper edge of the fault on the displacement field has also been studied numerically.

The results obtained in this paper are generalizations of our previous results (Rani and Singh, 2005), in the sense that the medium considered in the present work is orthotropic, which is more realistic than the isotropic medium. Although a 2-D model is a simplification of the physical system, such a model is useful in gaining insight into the relationship among various parameters.

Throughout most of California, earthquakes on the San Andreas fault may occur at the shallow depths of approximately 20 km (Brace and Byerlee, 1970). For the shallow earthquakes, the elastic layer of our problem may be identified with the topmost brittle region of the crust, and the welded elastic base with a crustal zone. The intermediate earthquakes of focal depths between 30 and 300 km have occurred in

Europe and elsewhere. The intermediate-depth shocks, ranging from 60 to 150 km in focal depth and with greater concentration, have been located near Granada and Malaga, Spain (Buforn et al., 1991). For the intermediate earthquakes, the model of the earth consisting of a lithosphere lying over an asthenosphere may be used. The ‘welded’ case of our problem together with the correspondence principle of linear viscoelasticity (Biot, 1954) may be used to study the intermediate earthquakes. The occurrence of deep shocks, at a depth of about 650 km below southern Spain, near Granada, is well-known. The earthquakes at great depths are fundamentally explosive in nature, involving sudden changes of volume rather than being the result of fracture involving shear (Richter, 1958).

It is well known that seismic waves radiate from faults. The Love waves may propagate in an elastic layer lying over a rigid base (Savarensky, 1975). The rigid base upon which the elastic layer lies is not absolutely rigid but may possess certain elasticity. It may be approximated to be rigid for some situations, such as for coal seam (taken as elastic layer) lying over the metamorphic rocks (taken as base). Coal seam is a class of sedimentary rocks and occurs in the Dawson County region of Montana. Krey (1963) was the first to use the Love waves to detect faults in coal seams.

Physically, the ‘smooth-rigid’ interface condition is applicable to the engineering problems, in which there is a possibility of a layer (such as a layer of petroleum materials) slipping over a base. This can also be used to study the effect of an internal horizontal boundary which is lubricated and the shear stress components and vertical component of the displacement vector become zero there.

The Palos Verdes fault is a long major strike-slip fault on the southwestern edge of the Los Angeles metropolitan area, with its slip in the sediments (Olsen and Archuleta, 1996). It has been established that an earthquake source lies in the Palaeozoic-type sedimentary rocks in Enola, Arkansas, USA (Crampin, 1994). Such sedimentary rocks may be represented in our model by a layer occupying the region  $0 \leq z < H$ , and the bottom of the layer, i.e.,  $z = H$ , may be taken as ‘rough-rigid’, so that the displacement vector becomes zero there (Small and Booker, 1984).

## ACKNOWLEDGEMENTS

Authors are thankful to the reviewers and to the Editor for their valuable suggestions on the improvement of the paper to its present form.

## REFERENCES

1. Aki, K. and Richards, P.G. (1980). “Quantitative Seismology: Theory and Methods, Volumes I and II”, W.H. Freeman and Company, San Francisco, U.S.A.
2. Ben-Menahem, A. and Singh, S.J. (1968). “Multipolar Elastic Fields in a Layered Half-Space”, *Bulletin of the Seismological Society of America*, Vol. 58, No. 5, pp. 1519–1572.
3. Biot, M.A. (1954). “Theory of Stress-Strain Relations in Anisotropic Viscoelasticity and Relaxation Phenomena”, *Journal of Applied Physics*, Vol. 25, No. 11, pp. 1385–1391.
4. Brace, W.F. and Byerlee, J.D. (1970). “California Earthquakes: Why Only Shallow Focus?”, *Science*, Vol. 168, No. 3939, pp. 1573–1575.
5. Buforn, E., Udias, A. and Madariaga, R. (1991). “Intermediate and Deep Earthquakes in Spain”, *Pure and Applied Geophysics*, Vol. 136, No. 4, pp. 375–393.
6. Burridge, R. and Knopoff, L. (1964). “Body Force Equivalents for Seismic Dislocations”, *Bulletin of the Seismological Society of America*, Vol. 54, No. 6A, pp. 1875–1888.
7. Bush, I. and Crampin, S. (1987). “Observations of EDA and PTL Anisotropy in Shear Wave VSPs”, *SEG Technical Program Expanded Abstracts*, Vol. 6, No. S11, pp. 646–649.
8. Chung, T.J. (1996). “Applied Continuum Mechanics”, Cambridge University Press, New York, U.S.A.
9. Crampin, S. (1989). “Suggestions for a Consistent Terminology for Seismic Anisotropy”, *Geophysical Prospecting*, Vol. 37, No. 7, pp. 753–770.
10. Crampin, S. (1994). “The Fracture Criticality of Crustal Rocks”, *Geophysical Journal International*, Vol. 118, No. 2, pp. 428–438.

11. Dziewonski, A.M. and Anderson, D.L. (1981). "Preliminary Reference Earth Model", *Physics of the Earth and Planetary Interiors*, Vol. 25, No. 4, pp. 297–356.
12. Fernández, J. and Rundle, J.B. (2004). "Postseismic Viscoelastic-Gravitational Half Space Computations: Problems and Solutions", *Geophysical Research Letters*, Vol. 31, No. 7, pp. L07608: 1–4.
13. Fukahata, Y. and Matsu'ura, M. (2006). "Quasi-Static Internal Deformation due to a Dislocation Source in a Multilayered Elastic/Viscoelastic Half-Space and an Equivalence Theorem", *Geophysical Journal International*, Vol. 166, No. 1, pp. 418–434.
14. Garg, N.R., Madan, D.K. and Sharma, R.K. (1996). "Two-Dimensional Deformation of an Orthotropic Elastic Medium due to Seismic Sources", *Physics of the Earth and Planetary Interiors*, Vol. 94, No. 1, pp. 43–62.
15. Hess, H.H. (1964). "Seismic Anisotropy of the Uppermost Mantle under Oceans", *Nature*, Vol. 203, No. 4945, pp. 629–631.
16. Kasahara, K. (1964). "A Strike-Slip Fault Buried in a Layered Medium", *Bulletin of the Earthquake Research Institute, University of Tokyo*, Vol. 42, No. 4, pp. 609–619.
17. Krey, T. (1963). "Channel Waves as a Tool of Applied Geophysics in Coal Mining", *Geophysics*, Vol. 28, No. 5, pp. 701–714.
18. Love, A.E.H. (1944). "A Treatise on the Mathematical Theory of Elasticity", Dover Publications, New York, U.S.A.
19. Madan, D.K. and Garg, N.R. (1997). "Static Deformation of an Orthotropic Horizontal Elastic Layer Coupling in Different Ways to a Base due to a Very Long Inclined Strike-Slip Fault Embedded in the Layer", *Indian Journal of Pure & Applied Mathematics*, Vol. 28, No. 5, pp. 697–712.
20. Maruyama, T. (1966). "On Two-Dimensional Elastic Dislocations in an Infinite and Semi-Infinite Medium", *Bulletin of the Earthquake Research Institute, University of Tokyo*, Vol. 44, No. 3, pp. 811–871.
21. Okada, Y. (1985). "Surface Deformation due to Shear and Tensile Faults in a Half-Space", *Bulletin of the Seismological Society of America*, Vol. 75, No. 4, pp. 1135–1154.
22. Okada, Y. (1992). "Internal Deformation due to Shear and Tensile Faults in a Half-Space", *Bulletin of the Seismological Society of America*, Vol. 82, No. 2, pp. 1018–1040.
23. Olsen, K.B. and Archuleta, R.J. (1996). "Three-Dimensional Simulation of Earthquakes on the Los Angeles Fault System", *Bulletin of the Seismological Society of America*, Vol. 86, No. 3, pp. 575–596.
24. Pan, E. (1989). "Static Response of a Transversely Isotropic and Layered Half-Space to General Dislocation Sources", *Physics of the Earth and Planetary Interiors*, Vol. 58, No. 2-3, pp. 103–117.
25. Rani, S. and Singh, S.J. (2005). "A Note on 2-D Lithospheric Deformation due to a Blind Strike-Slip Fault", *Journal of Earth System Science*, Vol. 114, No. 1, pp. 105–110.
26. Richter, C.F. (1958). "Elementary Seismology", W.H. Freeman and Company, San Francisco, U.S.A.
27. Rundle, J.B. (1980). "Static Elastic-Gravitational Deformation of a Layered Half Space by Point Couple Sources", *Journal of Geophysical Research*, Vol. 85, No. B10, pp. 5355–5363.
28. Rybicki, K. (1971). "The Elastic Residual Field of a Very Long Strike-Slip Fault in the Presence of a Discontinuity", *Bulletin of the Seismological Society of America*, Vol. 61, No. 1, pp. 79–92.
29. Rybicki, K. (1978). "Static Deformation of a Laterally Inhomogeneous Half-Space by a Two-Dimensional Strike-Slip Fault", *Journal of Physics of the Earth*, Vol. 26, No. 4, pp. 351–366.
30. Savarensky, E.F. (1975). "Seismic Waves", Mir Publishers, Moscow, Russia.
31. Singh, S.J. (1970). "Static Deformation of a Multilayered Half-Space by Internal Sources", *Journal of Geophysical Research*, Vol. 75, No. 17, pp. 3257–3263.
32. Singh, S.J. and Garg, N.R. (1985). "On Two-Dimensional Elastic Dislocations in a Multilayered Half-Space", *Physics of the Earth and Planetary Interiors*, Vol. 40, No. 2, pp. 135–145.
33. Small, J.C. and Booker, J.R. (1984). "Finite Layer Analysis of Layered Elastic Materials Using a Flexibility Approach. Part 1—Strip Loadings", *International Journal for Numerical Methods in Engineering*, Vol. 20, No. 6, pp. 1025–1037.

34. Talebian, M., Fielding, E.J., Funning, G.J., Ghorashi, M., Jackson, J., Nazari, H., Parsons, B., Priestley, K., Rosen, P.A., Walker, R. and Wright, T.J. (2004). "The 2003 Bam (Iran) Earthquake: Rupture of a Blind Strike-Slip Fault", *Geophysical Research Letters*, Vol. 31, No. 11, pp. L11611: 1–4.
35. Verma, R.K. (1960). "Elasticity of Some High-Density Crystals", *Journal of Geophysical Research*, Vol. 65, No. 2, pp. 757–766.
36. Wang, R., Martin, F.L. and Roth, F. (2003). "Computation of Deformation Induced by Earthquakes in a Multi-layered Elastic Crust—FORTRAN Programs EDGRN/EDCMP", *Computers & Geosciences*, Vol. 29, No. 2, pp. 195–207.
37. Wang, R., Martin, F.L. and Roth, F. (2006). "PSGRN/PSCMP—A New Code for Calculating Co- and Post-Seismic Deformation, Geoid and Gravity Changes Based on the Viscoelastic-Gravitational Dislocation Theory", *Computers & Geosciences*, Vol. 32, No. 4, pp. 527–541.